Ni$_x$Co$_{3-x}$O$_4$ 表面修饰对 CdSe/TiO$_2$ 纳米管阵列光电化学氧化水活性的影响

许 贞 [1,2] 李 娟 [1] 李新军 *,[1]

(^{1} 中国科学院可再生能源与天然气水合物重点实验室,
中国科学院广州能源研究所, 广州 510640)
(^{2} 中国科学院大学, 北京 100049)

摘要: 利用氨挥发诱导法在 CdSe/TiO$_2$ 纳米管阵列表面负载一层 Ni$_x$Co$_{3-x}$O$_4$。采用 SEM、XRD、XPS、UV-Vis 对样品进行表征,通过线性扫描伏安法测定光阳极的释氧电势来评价其光电水氧化活性。结果表明:表面 Ni$_x$Co$_{3-x}$O$_4$ 是尖晶石结构;相对于 CdSe/TiO$_2$ 纳米管阵列光阳极, Ni$_x$Co$_{3-x}$O$_4$/CdSe/TiO$_2$ 光阳极能将光电氧化水的过电势降低 430 mV。Ni 离子的引入使得 Ni$_x$Co$_{3-x}$O$_4$ 表面富含三价阳离子(Ni^{3+}, Co^{3+}),从而促进 CdSe/TiO$_2$ 光阳极光电水氧化的进行。

Effect of Ni$_x$Co$_{3-x}$O$_4$ Modification for CdSe/TiO$_2$ Nanotube Arrays on Activity of Photoelectrochemical Oxidation of Water

XU Zhen[1,2]   LI Juan[1]   LI Xinjun*,[1]

(^{1}*Key Laboratory of Renewable Energy and Gas Hydrate, Guangzhou Institute of Energy Conversion,*
Chinese Academy of Sciences, Guangzhou 510640, *China*)
(^{2}*University of Chinese Academy of Sciences, Beijing* 100049, *China*)

Abstract: CdSe/TiO$_2$ nanotube array (TiO$_2$NTA) film was modified by Ni$_x$Co$_{3-x}$O$_4$ through the method of ammonia-evaporation induction growth. The films were characterized by X-ray diffraction, field emission scanning electron microscopy, energy dispersive spectroscopy, X-ray photoelectron spectroscopy and UV-Vis diffuse reflectance spectroscopy. To characterize the photoanodes activity of photoelectrochemical oxidation of water, the chopped linear sweep voltammetry was performed in a three-electrode system under simulated solar irradiation. The results show that CdSe/TiO$_2$NTA is covered by a thin layer of Ni$_x$Co$_{3-x}$O$_4$ with the spinel structure in which Ni and Co are both in divalent and trivalent states. The modification of Ni$_x$Co$_{3-x}$O$_4$ on the CdSe/TiO$_2$NTA can lower the overpotential of water oxidation by about 430 mV compared with the CdSe/TiO$_2$NTA. The introduction of Ni into the structure of Co$_3$O$_4$ leads to the surface enhancement of trivalent cations (Ni^{3+} and Co^{3+}) and consequently facilitates the oxidation of water.

Key words: TiO$_2$ nanotube arrays; CdSe; Ni$_x$Co$_{3-x}$O$_4$; ammonia-evaporation induction growth; photoelectrochemical oxidation of water

0　Introduction

Solar splitting of water into hydrogen is a promising industrial photosynthesis process that would provide clean fuel[1-2]. But the low efficiency of solar water splitting greatly limits its application. In order to improve the efficiency, numerous efforts have been devoted to developing new materials with visible light excitation such as the N doped TiO_2 [3], sulfur-substituted and zinc-doped $In(OH)_3$[4], $Ga_{1-x}Zn_xO_{1-x}N_x$[5-6], $Cu_xCd_{1-x}S$ [7], ZnS/CuS porous nanosheets[8], ZnS-CdS/SiO_2 [9] and $ZnS-In_2S_3-Ag_2S$ [10]. Besides, the TiO_2 nanotube draws great attention because of its high energy conversion efficiency such as Au/TiO_2 nanotube arrays [11]. Our previous work [12] has shown that the CdSe sensitized TiO_2 nanotube composite is a good visible light harvesting material with improved electron transporting property. On the other hand, from the perspective of dynamics co-loading catalysts like hydrogen evolution catalysts (HECs) or oxygen evolution catalysts (OECs) can promote the water reduction or the water oxidation in order to enhance solar water splitting efficiency [13]. Successful water reduction has been reported and can be promoted by hydrogen evolution co-catalysts such as Pt, $Ni(OH)_2$[14] and $Cu(OH)_2$ [15]. However, in the water splitting process, the four electrons and four protons transfer make the oxidation of water much more difficult than the reduction of water with a two-electron process. As a result, water oxidation is always considered as the bottleneck in the overall water splitting [16]. Proper OECs can serve as the oxidation sites to decrease the overpotential of water oxidation [13], which motivates intensified research on pursuing efficient OECs[16].

Much effort about the OECs has been made in water electrolysis. IrO_2 and RuO_2 in acidic conditions and spinel-structured Co_3O_4 as well as perovskite-structured metal oxides ($NiLa_2O_4$ and $LaCoO_3$) in basic conditions have been used to catalyze oxygen evolution reaction (OER) with moderate overpotentials (about 300~400 mV)[1,17]. Some research works indicate that suitable materials, which are used as electrocatalysts (such as IrO_2, RuO_2, cobalt phosphate

and nickel borate), can improve oxygen evolution kinetics when coupled with semiconductor photocatalysts[18-23]. Especially, cobalt/nickel-containing co-catalysts with the easy accessibility in nature are considered as the most promising OEC materials. Recently, Zhang[16] has reported that the integrating of Co_3O_4 into carbon nitride nanohybrids can promote charge separation and lower the overpotential of water oxidation. Moreover, Li [24] has reported that the $Ni_xCo_{3-x}O_4$ nanowire array electrode has much higher current density at the same potential and shows higher electrocatalytic activity in water oxidation than the Co_3O_4. Enlightened by these works, we consider that $Ni_xCo_{3-x}O_4$ would be an effective OEC in solar water oxidation.

Herein, based on the previous work of constructing $CdSe/TiO_2NTAs$, we further fabricated a $Ni_xCo_{3-x}O_4/CdSe/TiO_2NTAs$ photoanode composite by depositing $Ni_xCo_{3-x}O_4$ on $CdSe/TiO_2NTAs$ using ammonia-evaporation induction growth method[25-26]. The effect of $Ni_xCo_{3-x}O_4$ modification for the $CdSe/TiO_2NTAs$ films on the water oxidation activity was investigated by the photoelectrochemical characterization.

1　Experimental

1.1　Materials

Ti foil (250 μm thick, 99.5% purity) was purchased from Shenzhen City Xuguang Titanium Co., LTD. Hydrofluoric acid (HF), nitrate acid (HNO_3), aqueous ammonia (25wt%) and anhydrous ethanol (CH_3CH_2OH) were obtained from Guangzhou Chemical Reagent Factory. Nickel nitrate ($Ni(NO_3)_2 \cdot 6H_2O$), cobalt nitrate ($Co(NO_3)_2 \cdot 6H_2O$), selenium oxide (SeO_2), cadmium sulfate octahydrate ($3CdSO_4 \cdot 8H_2O$) and sulfuric acid (H_2SO_4) were purchase from Guangzhou Guanghua Chemical Factory Co., LTD. All the reagents were of analytical grade and used as received.

1.2　Preparation

The $CdSe/TiO_2NTAs$ were prepared following the typical procedure [12]. The ordered TiO_2NTAs were obtained in a HF solution using anodic oxidation. Deposition of CdSe nanoparticles were carried out by

ultrasonic-assisted cyclic voltammetry electrochemical deposition process. It was deposited for 60 cycles under the potential from −0.40 V to −0.85 V through cyclic voltammograms with constantly ultrasonic. The samples were thoroughly rinsed by distilled water and then dried in the air. Finally the samples were annealed at 350 ℃ in N$_2$ atmosphere for 60 min.

The fabrication of $Ni_xCo_{3-x}O_4$/CdSe/TiO$_2$NTAs film was achieved via the ammonia-evaporation induction growth. 5 mmol Ni(NO$_3$)$_2$·6H$_2$O and 5 mmol Co(NO$_3$)$_2$·6H$_2$O were dissolved in 100 mL distilled water, and then 30 mL ammonia (25wt%) was added dropwise to form a clear solution. The solution was continuously stirred for half an hour before it was transferred to a petri dish. The CdSe/TiO$_2$ NTAs film substrate was placed in the dish with the interested side down, which was approximately 1~2 mm away from the bottom of the dish. Then the solution was sealed and placed in a pre-heated oven at 100 ℃ for 2 h. The as-prepared composite film was thoroughly washed with distilled water and then dried in air at 70 ℃, and finally annealed at 250 ℃ in the air for 2 h. Co$_3$O$_4$/CdSe/TiO$_2$NTAs and NiO/CdSe/TiO$_2$NTAs were also prepared according to the aforementioned procedure except that the precursor solution of the former contained 10 mmol Co(NO$_3$)$_2$·6H$_2$O and the one of the latter contained 10 mmol Ni(NO$_3$)$_2$·6H$_2$O.

1.3　Characterization

The morphology of the films was observed using a field emission scanning electron microscope (FESEM, Hitachi S-4800) equipped with a detector for energy dispersive spectroscopy (EDS).

The crystalline phase of the films was investigated by X-ray diffraction (XRD, X′Pert-PRO, PANalytical, Holland) with Cu $K\alpha1$ radiation ($\lambda = 0.154\ 056$ nm) at an accelerating voltage of 40 kV and a current of 40 mA. The patterns were recorded in the 2θ range from 10° to 80° at a scan rate of 1.5°·min^{-1}.

The different states of elements were studied with X-ray photoelectron spectroscopy analysis (XPS, Kratos XSAM800 X-ray photoelectron spectrometer, England) using Al $K\alpha$ irradiation at 180 W (12 kV,

15 mA). The spectra were collected at a fixed analyzer pass energy of 20 eV, and all binding energy values were calibrated to C1s=284.6 eV.

The diffuse reflectance spectra (DRS) of films were recorded by a UV-Vis spectrophotometer (LAMBDA 750) equipped with an integrating sphere and with BaSO$_4$ as a reference in the range of 300~700 nm. The width of slit was 5.0 nm and the step was 0.5 nm.

1.4　Photoelectrochemical measurements

All the photoelectrochemical measurements were performed in a three-electrode electrochemical cell with a quartz window under the illumination of a 300 W xenon lamp at room temperature. Linear sweep voltammetry (LSV) was employed in the three-electrode system which was linked with CHI660A electrochemical station.

The chopped LSV was conducted with a scan rate of 3 mV·s^{-1} and a chopped frequency of 0.2 Hz. The $Ni_xCo_{3-x}O_4$/CdSe/TiO$_2$NTAs film, a platinum sheet, and a saturated calomel electrode (SCE) served as working electrode, counter electrode and reference electrode, respectively. The working electrode was mounted in a special holder with an area of 3 cm^2 exposed to a quartz window. All photoelectrochemical experiments were conducted in a 1 mol·L^{-1} NaOH aqueous solution.

2　Results and discussion

2.1　SEM and EDS analysis

Fig.1 shows the SEM images of TiO$_2$NTAs, CdSe/TiO$_2$NTAs and $Ni_xCo_{3-x}O_4$/CdSe/TiO$_2$NTAs. The diameters of the TiO$_2$NTAs are about 80 nm (Fig.1a). The nanosized CdSe particles are deposited onto the TiO$_2$NTAs. Many of the particles are embedded in the TiO$_2$ nanotubes which can utilize most of the surface area (Fig.1b). After the deposition of the $Ni_xCo_{3-x}O_4$, the CdSe particles are almost totally covered by the $Ni_xCo_{3-x}O_4$ layer (Fig.1c). The existence of the Ni is verified by the EDS method as shown in Fig.1d. The EDS analysis exhibits that the molar ratio of Co/Ni is about 2.8 for $Ni_xCo_{3-x}O_4$/CdSe/TiO$_2$NTAs sample. So it can be inferred that the composition of $Ni_xCo_{3-x}O_4$ is
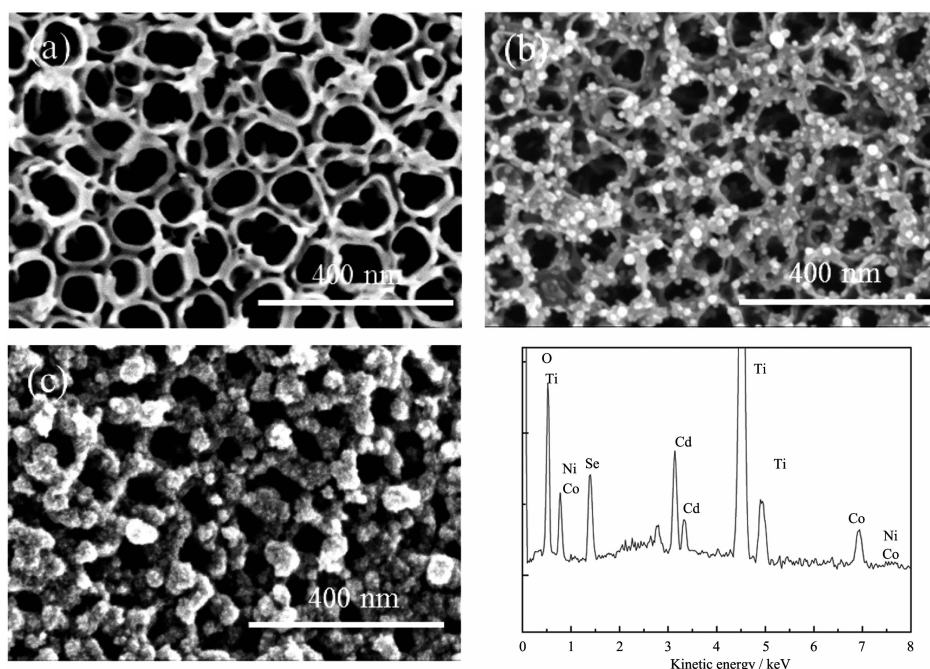
Fig.1　SEM image of TiO$_2$NTAs (a), CdSe/ TiO$_2$NTAs (b), Ni$_x$Co$_{3-x}$O$_4$/CdSe/TiO$_2$NTAs (c), EDS　of Ni$_x$Co$_{3-x}$O$_4$/CdSe/TiO$_2$NTAs (d)

most likely to be Ni$_{0.8}$Co$_{2.2}$O$_4$.

2.3　XRD analysis

Fig.2 shows XRD patterns of CdSe/TiO$_2$NTAs, Co$_3$O$_4$/CdSe/TiO$_2$NTAs and Ni$_x$Co$_{3-x}$O$_4$/CdSe/TiO$_2$NTA samples. The three samples show anatase peak at 2θ of 25.3° corresponding to the planes　(101). After the deposition of CdSe, the main diffraction peak at 2θ of 42.1° emerges, which is attributed to CdSe (220) plane. Finally with the loading of Ni$_x$Co$_{3-x}$O$_4$ and Co$_3$O$_4$, spinel peak of the plane　(311) at 2θ of 36.7° appears.

2.3　XPS analysis

Fig.3 shows XPS spectra of Ni2p, Co2p and O1s in the Ni$_x$Co$_{3-x}$O$_4$/CdSe/TiO$_2$NTAs sample. In Fig.3a,

the 2$p_{3/2}$ binding energy at 854.3 eV is characteristic of Ni^{2+}, while the one at 856.3 eV is assigned to Ni^{3+},
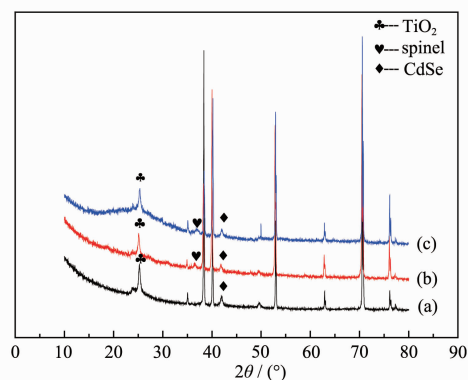

Fig.2　XRD patterns of CdSe/TiO$_2$NTAs (a), Co$_3$O$_4$/CdSe/ TiO$_2$NTAs (b), Ni$_x$Co$_{3-x}$O$_4$/CdSe/TiO$_2$NTAs (c)
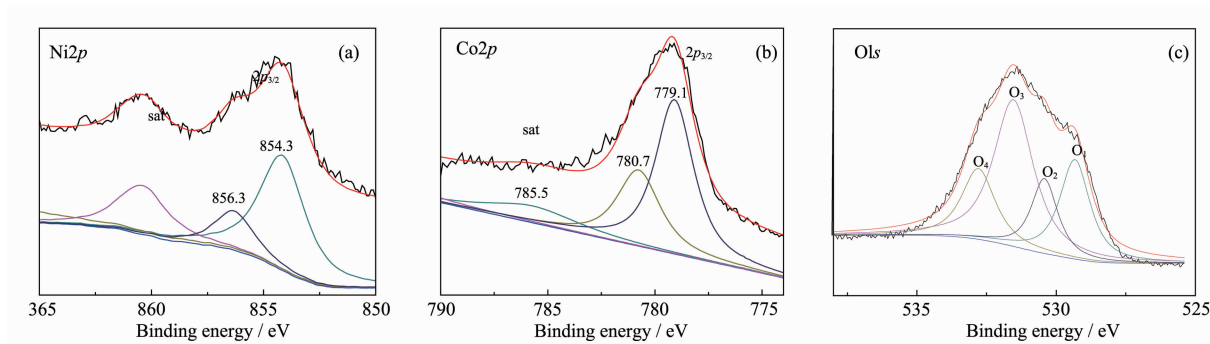

Fig.3　Typical XPS high-resolution spectra (top) together with deconvoluted peaks (bottom) of Ni2p (a), Co2p (b), O1s (c) in the sample of Ni$_x$Co$_{3-x}$O$_4$/CdSe/TiO$_2$NTAs

indicating that Ni element is present at the surface in the form of both Ni^{2+} and Ni^{3+} ions [27]. The intensity ratio of Ni^{3+}/Ni^{2+} in the summation spectrum is about 0.23. From Fig.3b, it can be seen that the cobalt exhibit $2p_{3/2}$ binding energy level at 779.1 eV and 780.7 eV[28], which are characteristic of the octahedral Co^{3+} and the tetrahedral Co^{2+} with a intensity ratio of 2.38. The O1s spectrum can be deconvoluted into four contributions as shown in Fig.3c. Component O1 at 529.3 eV is typical of metal-oxygen bond [29]. Component O2 at 530.4 eV is characteristic of oxygen in OH groups, indicating that the surface is hydroxylated to some extent as a result of the presence of CoOOH and/or NiOOH which is in accordance with the deduction of Roginskaya and Gautier[30-31]. Gerken[32] considers it to be reasonable to expect that the surfaces of spinel-type materials can be restructured into layered double hydroxide type structures during water oxidation process. Recently, Yeo and Bell [33] have verified this type of restructuration using in-situ Raman spectroscopy. Contribution O3 located at 531.5 eV is associated with oxygen ions in low coordination on the surface. Finally, component O4 at 532.7 eV can be attributed to surface bond water.

2.4　UV-Vis absorption spectra

　　Fig.4 shows the diffuse reflection spectra (DRS) of CdSe/TiO$_2$NTAs, Co$_3$O$_4$/CdSe/TiO$_2$NTAs, NiO/CdSe/ TiO$_2$NTAs and Ni$_x$Co$_{3-x}$O$_4$/CdSe/TiO$_2$NTAs composites. The band gap absorption edge of CdSe/TiO$_2$NTAs is
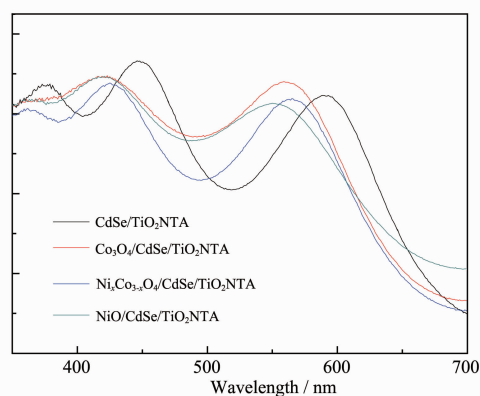
Fig.4　Diffuse reectance spectra of CdSe/TiO$_2$NTAs (a), Co$_3$O$_4$/CdSe/TiO$_2$NTAs (b), Ni$_x$Co$_{3-x}$O$_4$/ CdSe/ TiO$_2$NTAs (c), NiO/CdSe/TiO$_2$NTAs (d)

about 650 nm. After the deposition of Co$_3$O$_4$, NiO and Ni$_x$Co$_{3-x}$O$_4$, the maximum peaks of the DRS curves have a slight blue shift. The changes of DRS curves may be attributed to bigger band gap of the surface materials. The band gap of Co$_3$O$_4$, NiO and Ni$_x$Co$_{3-x}$O$_4$ are about 2.07 eV [34], 3.6 eV [35] and 2.06 eV [36], respectively which are all bigger than that of CdSe (1.7 eV). Considering the whole absorption region, the surface modification layers have a very little effect on the absorption of the composites. These surface modification materials mainly serve as the OER co-catalysts.

2.5　Photoelectrochemical behavior

　　Fig.5 shows linear sweeping voltammetry (LSV) of the parent CdSe/TiO$_2$NTAs and the composite photoanodes with different modifications in 1 mol·L^{-1} NaOH aqueous solution under simulated sunlight illumination. It can be seen that the photocurrents increase in various degrees after the surface modification, which is mainly attributed to the enhancement of separation of charge-carriers at the external electric field [37]. The potential where the current begins to have a sharp increase in the chopped LSV plots is defined as the onset potential for water oxidation as marked by the arrow. It can be observed that the potentials for water oxidation are
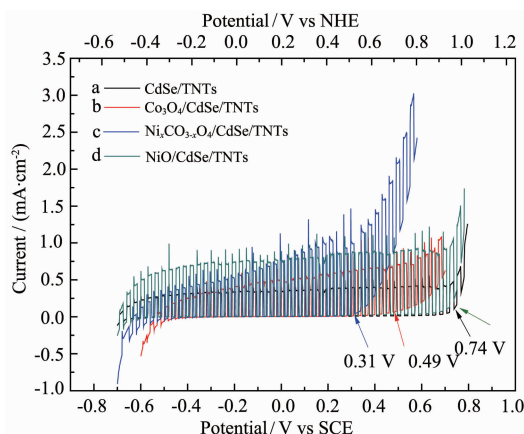
Fig.5　Photocurrent-potential characteristics of CdSe/ TiO$_2$NTAs (a), Co$_3$O$_4$/CdSe/TiO$_2$NTAs (b), Ni$_x$Co$_{3-x}$O$_4$/CdSe/TiO$_2$NTAs (c), NiO/CdSe/ TiO$_2$NTAs (d) measured (scan rate, 3 mV·s^{-1}) with chopped light (0.2 Hz). The arrows in the figure indicate the onset potential of water oxidation

0.98 V, 0.98 V, and 0.73 V, 0.56 V (vs NHE) for CdSe/TiO$_2$NTAs, NiO/CdSe/TiO$_2$NTAs, Co$_3$O$_4$/CdSe/ TiO2NTAs and Ni$_x$Co$_{3-x}$O$_4$/CdSe/TiO$_2$NTAs, respectively. It is demonstrated that the Co$_3$O$_4$ modification cathodically shifts the onset potential for water oxidation by 250 mV and the Ni$_x$Co$_{3-x}$O$_4$ modification further shifts this potential by about 430 mV, when compared to that of CdSe/TiO$_2$NTAs. Although NiO can increase the photocurrent, it indeed has little effect on reducing the overpotential for water oxidation (Fig.5d). Hence NiO with Ni in divalent oxidation state is not an effective OEC. In the Ni-Bi OEC system, Ni with an avenge oxidation state between Ni^{III} and Ni^{IV} has good oxygen evolution activity[38].

2.6 The possible process of water oxidation on Ni$_x$Co$_{3-x}$O$_4$/CdSe/TiO$_2$NTAs

Because of an efficient harvesting of visible light and high electron transport property [12], CdSe/ TiO$_2$NTAs composite is a promising material for photoelectrochemical water splitting. Theoretically, the potential for water oxidation in 1 mol·L^{-1} NaOH solution is 0.40 V vs NHE (E_{anode} / V=1.23−0.059pH vs NHE). In fact, the CdSe/TiO$_2$NTAs can only achieve the water oxidation with the bias above 0.98 V vs NHE (0.74 V vs SCE), as shown in Fig.5. Therefore, it suffers a big overpotential to drive water oxidizing into oxygen under the condition of photoelectrochemical water splitting. With a reduced overpotential, it would be much easier to proceed for the water oxidation reaction.

After the modification of Co$_3$O$_4$ on the CdSe/ TiO$_2$NTAs photoanode, the potential for water oxidation is decreased to 0.73 V vs NHE (0.49 V vs SCE) in our experiment, with a cathodic shift by 250 mV compared with that of CdSe/TiO$_2$NTAs. Feng Jiao and co-workers [39] have reported that Co$_3$O$_4$ can decrease the overpotential for water oxidation. In their work, nanostructured Co$_3$O$_4$ clusters in mesoporous silica can achieve efficient water oxidation driven by visible light-generated [Ru^{3+}(bpy)$_3$] under the modest overpotential of 350 mV.

The overpotential of the Ni$_x$Co$_{3-x}$O$_4$/CdSe/TiO$_2$NTAs photoanode is cathodically shifted by about 430 mV

and 180 mV relative to the CdSe/TiO$_2$NTAs photoanode and Co$_3$O$_4$/CdSe/TiO$_2$NTAs photoanode, respectively, as shown in Fig 5. In water electrolysis, Ni$_x$Co$_{3-x}$O$_4$ on titanium plates was observed to evolve oxygen at lower overpotential as compared to that of Co$_3$O$_4$ [40]. The electrochemically created tetravalent cations from trivalent cations are considered to be active sites for OER [24,41-42]. Therefore, it is suggested that the quantity of trivalent cation sites on the surface and the facile formation of tetravalent cations are of importance to the oxygen evolution reaction.

The synergic effects of the Ni and Co in the structure of Ni$_x$Co$_{3-x}$O$_4$ bring about a possible increase of trivalent cation sites (Co^{3+} or Ni^{3+}) on the surface in comparison to Co$_3$O$_4$, as verified by XPS studies in Fig.3. Usually spinel-structured Co$_3$O$_4$ has octahedrally coordinated Co^{3+} and tetrahedrally coordinated Co^{2+}[27]. Godinho [43] and other researchers think that the incorporation of Ni into the Co$_3$O$_4$ would bring about the presence of tetrahedrally coordinated Co^{3+} in addition to the original octahedral Co^{3+} sites. Tetrahedrally coordinated Co^{3+} sites locate more closely to the surface and thus can intimately interact with oxygen species and favor of the water oxidation reaction. On the other hand, the Co ion can also affect the oxidation state of the Ni ions in the structure of Ni$_x$Co$_{3-x}$O$_4$. A small part of Ni would probably substitute for the Co^{3+} and exist as Ni^{3+}. The synergetic effect between Co and Ni can increase the activity and reversibility of the Ni^{II}/Ni^{III} [44], and thus result in the facile formation of Ni^{III}. The surface trivalent cations may exist as the MOOH (M=Co, Ni) which can be deduced by our XPS study. And MOOH (M = Co and Ni) is supposed to be the "right type of oxide" for the OER [45]. Moreover, in the water oxidation, the facile oxidation from M^{III} to M^{IV} is also very important, because the tetravalent cations (M^{IV}) can serve as the active sites of oxygen evolution. The existence of Ni can make the Co^{III}/Co^{IV} transition happen at more negative potential [46], which in turn can achieve oxygen evolution at lower overpotential on the site of Co^{IV}. Furthermore, the oxidation of Ni^{III}/Ni^{IV} proceeds at lower potential than that of Co^{III}/Co^{IV}. Thus

the existence of Ni^{IV} can further decrease the overpotential and increase the activity for water oxidation.

The mechanistic proposal for water photooxidation on the surface of $Ni_xCo_{3-x}O_4/CdSe/TiO_2NTAs$ is summarized schematically in Fig.6. M^{III} of MOOH on the surface captures holes from the valence band of CdSe created by visible light illumination, and then gets oxidized into M^{IV} which further participate in the oxygen evolution reaction. At the same time, electrons from the conduction band of CdSe transport to external circuit passing through the TiO_2NTAs to participate in the water reduction process at the other electrode.
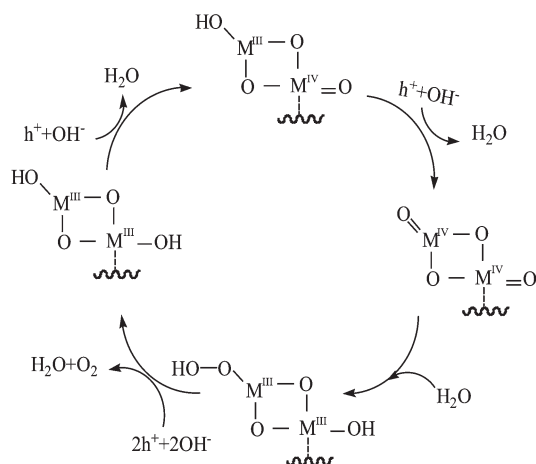

Fig.6　Schematic procedure of water oxidation by
$Ni_xCo_{3-x}O_4/CdSe/TiO_2NTAs$

3　Conclusions

In summary, we fabricate a $Ni_xCo_{3-x}O_4/CdSe/TiO_2NTAs$ photoanode composite by depositing $Ni_xCo_{3-x}O_4$ on $CdSe/TiO_2NTAs$ via ammonia-evaporation induction growth method. The $Ni_xCo_{3-x}O_4/CdSe/TiO_2NTAs$ photoanode shows a decrease in overpotential of about 430 mV and 180 mV compared with $CdSe/TiO_2NTAs$ photoanode and $Co_3O_4/CdSe/TiO_2NTAs$ photoanode, implying a higher activity for water oxidation. The introduction of Ni into the structure of Co_3O_4 could bring about the surface enhancement of trivalent cations (Ni^{3+} and Co^{3+}) and the more facile formation of tetravalent cations (Ni^{4+} and Co^{4+}) during the photoelectrochemical oxidation of water, and consequently facilitate the process of

water oxidation.

References:

[1] Walter M G, Warren E L, Lewis N S, et al. *Chem. Rev.*, **2010**,**110**:6446-6473

[2] SHANGGUAN Wen-Feng(上官文峰). *Chinese J. Inorg. Chem.*(*Wuji Huaxue Xuebao*), **2001**,**17**:620-626

[3] Asahi R, Morikawa T, Ohwaki T, et al. *Science*, **2001**,**293**: 269-271

[4] Lei Z, Ma G, Li C, et al. *J. Catal.*, **2006**,**237**:322-329

[5] Maeda K, Takata T, Domen, K, et al. *J. Am. Chem. Soc.*, **2005**,**127**:8286-8287

[6] Maeda K, Domen K. *J. Phys. Chem. C*, **2007**,**111**:7851-7861

[7] CUI En-Tian(崔恩田), LÜ Gong-Xuan(吕功煊). *Chinese J. Inorg. Chem.*(*Wuji Huaxue Xuebao*), **2010**,**26**:2143-2149

[8] Zhang J, Yu J, Zhang Y, et al. *Nano Lett.*, **2011**,**11**:4774-4779

[9] ZHOU Peng(周鹏), LÜ Gong-Xuan(吕功煊), MA Jian-Tai(马建泰). *J. Mol. Catal.*(*China*)(*Fenzi Cuihua*), **2011**,**25**:328-335

[10]Li Y, Chen G, Zhou C, et al. *Chem. Commun.*, **2009**:2020-2022

[11]Xu Z, Yu J, Liu G. *Electrochem. Commun.*, **2011**,**13**:1260-1263

[12]Ouyang J L, Chang M L, Li X J, et al. *Thin Solid Films*, **2012**,**520**:2994-2999

[13]Hara M, Nunoshige J, Domen K, et al. *Chem. Commun.*, **2003**:3000-3001

[14]Ran J, Yu J, Jaroniec M. *Green Chem.*, **2011**,**13**:2708-2713

[15]Yu J, Ran J. *Energy Environ. Sci.*, **2011**,**4**:1364-1371

[16]Zhang J, Grzelczak M, Wang X, et al. *Chem. Sci.*, **2012**,**3**: 443-446

[17]Liang Y, Li Y, Dai H, et al. *Nat. Mater.*, **2011**,**10**:780-786

[18]Harriman A, Pickering I J, Thomas J M, et al. *J. Chem. Soc., Faraday Trans.* 1, **1988**,**84**:2795-2806

[19]Hong Y R, Liu Z, Al-Bukhari S F B S A, et al. *Chem. Commun.*, **2011**,**47**:10653-10655

[20]Steinmiller E M P, Choi K S. *Proc. Natl. Acad. Sci. U. S. A.*, **2009**,**106**:20633-20636

[21]Zhong D K, Choi S, Gamelin D R. *J. Am. Chem. Soc.*, **2011**, **133**:18370-18377

[22]Zhong D K, Sun J W, Gamelin D R, et al. *J. Am. Chem. Soc.*, **2009**,**131**:6086-6087

[23]Seabold J A, Choi K S. *Chem. Mat.*, **2011**,**23**:1105-1112

[24]Li Y, Hasin P, Wu Y. *Adv. Mater.*, **2010**,**22**:1926-1929

[25]Xia X, Tu J, Wang X, et al. *J. Mater. Chem.*, **2011**,**21**:9319-9325

[26]Xia X, Tu J, Wang X, et al. *RSC Adv.*, **2012,2**:1835-1841

[27]Oku M, Hirokawa K. *J. Solid State Chem.*, **1979,30**:45-53

[28]Chuang T, Brundle C, Rice D. *Surf. Sci.*, **1976,59**:413-429

[29]Choudhury T, Saied S, Abbot A M, et al. *J. Phys. D: Appl. Phys.*, **1989,22**:1185-1195

[30]Roginskaya Y E, Morozova O, Trasatti S, et al. *Langmuir*, **1997,13**:4621-4627

[31]Gautier J, Rios E, Gracia M, et al. *Thin Solid Films*, **1997, 311**:51-57

[32]Gerken J B, McAlpin J G, Stahl S S, et al. *J. Am. Chem. Soc.*, **2011,133**:14431-14442

[33]Yeo B S, Bell A T. *J. Am. Chem. Soc.*, **2011,133**:5587-5593

[34]Long M, Cai W, Cai J, et al. *J. Phys. Chem. B*, **2006,110**: 20211-20216

[35]Puspharajah P, Radhakrishna S, Arof A. *J. Mater. Sci.*, **1997,32**:3001-3006

[36]Cui B, Lin H, Liu Y, et al. *J. Phys. Chem. C*, **2009,113**: 14083-14087

[37]Xu Z, Yu J. *Nanoscale*, **2011,3**:3138-3144

[38]Risch M, Klingan K, Dau H, et al. *Chem. Commun.*, **2011, 47**:11912-11914

[39]Jiao F, Frei H. *Angew. Chem. Int. Ed.*, **2009,48**:1841-1844

[40]Singh R N, Koenig J F, Poillerat G, et al. *J. Electrochem. Soc.*, **1990,137**:1408-1413

[41]Kay A, Cesar I, Grätzel M. *J. Am. Chem. Soc.*, **2006,128**: 15714-15721

[42]Hibbert D B, Churchill C R. *J. Chem. Soc. Faraday Trans. 1*, **1984,80**:1965-1975

[43]Godinho M I, Catarino M A, Pereira M I, et al. *Electrochim. Acta*, **2002,47**:4307-4314

[44]Wu G, Li N, Zhou D R, et al. *J. Solid State Chem.*, **2004,177**:3682-3692

[45]Lyons M E, Brandon M P. *Int. J. Electrochem. Sci.*, **2008,3**: 1386-1424

[46]Hu C C, Lee Y S, Wen T C. *Mater. Chem. Phys.*, **1997,48**: 246-254